Effect of Surface Properties of Supported Pt-Based Catalysts on the Hydrogenation of N-(2`,3`-dimethoxybenzyl)-3,4-Dioxy-Methylene-Phenylethylamine

Guosheng Wang*, Tiantian zhang, Henan Yang, Xiaoguang San and Yingpeng Xie

Department of Chemical Engineering, Shenyang university of chemical technology, China

ABSTRACT

Pt/ Al_2O_3, Pt/Al_2O_3-xMgO and Pt/MgO catalysts were studied for hydrogenation of N-(2`,3`-dimethoxy benzyl)-3,4-dioxy-methylene-phenylethylamine, the N_2 physi-sorption, X-ray Diffraction (XRD), Carbon Dioxide Temperature Programmed Desorption (CO_2-TPD), Transmission Electron Microscopy (TEM), Temperature Programmed Reduction of Hydrogen (H_2-TPR), and X-ray Photoelectron Spectrometer (XPS) were used to study the physical properties of the catalysts, the surface acidity or basicity of the support, the interaction of active particles with support, the reducibility, dispersion, and active surface area of Pt for the Pt/ Al_2O_3, Pt/ Al_2O_3-xMgO and Pt/MgO catalysts. It was founded that the basic support (MgO) caused the electron deficient surface metallic Pt that favored the hydrogenation of N-(2`,3`-dimethoxy benzyl)-3,4-dioxy-methylene-phenylethylamine, and the mesoporosity of MgO support was benefit for the transport of large molecules reactants and products. The utilization of meso-porous Pt/MgO for catalytic hydrogenation of N-(2`,3`-dimethoxy benzyl)-3,4-dioxy-methylene-phenylethylamine (Shiff`s base) with the highest conversion of 96.74%, the highest selectivity of 95.25% and yields of 92.14% implied that the instead of Raney Ni was feasible.

Keywords: Pt/MgO, Hydrogenation, Mesoporosity, Basic support

INTRODUCTION

Raney nickel catalysts were widely used for much more chemical processes, such as (de)hydrogenation, catalytic activity, and strong stability. As a hydrogenation catalysts, it has been successfully applied to the chemical process such as hydrogenation of carbonyl, carboxyl, carbon-nitrogen bond, carbon-oxygen bond et.al., by now, Raney nickel was still used as catalysts for hydrogenation of N-(2`,3`-dimethoxy benzyl)-3,4-dioxy-methylene-phenylethylamine, which was raw materials or intermediates for synthesis of berberine.

Pt-based alumina supported catalysts (Pt/ Al_2O_3) possess high stability, activity, and/or selectivity, it has been successfully applied to the aqueous-phase reforming(APR) of polyols [1,2], hydrogenation of alkenes [3], NO oxidation [4], etc., the factors effected on the electronic properties of the catalysts had been studied such as the platinum oxide (PtOx) species, a weakly π-bonded or more strongly di-σ-bonded form, the support acid/base properties [5], or organometallic compounds [6].

Platinum supported on MgO (Pt/MgO) catalysts lies in the essentially basic surface character had been used in Claisen-Schmidt condensation [7], the partial oxidation of methane [8], hydrodeoxygenation (HDO) [9], hydroisomerization of n-hexadecane [10], propane dehydrogenation [11], NOx storage reduction (NSR) [12], etc., different source of platinum on the metal and surface properties [13,14], magnesium deficiency [15], the interaction of Pt on MgO [16,17], the formation of bulk oxide (Pt_3O_4, α-PtO_2) [18], hydrogen absorbed in MgO(100) [19,20], CO oxidation [21], had been studied by experimental or theoretical calculation.

The adsorption, surface reactions, and surface interactions on the Pt particle or clusters and acid and/or basic support had been investigated [22-28], the support included Al_2O_3, basic metal oxides, especially alkaline earth metal oxides, and sometimes binary metal oxides. It was implied that the metal oxides provide a distribution of strengths of Lewis

acid sites as well as strengths and types of basic sites which afford insight into the role of these various sites in reactants/metal oxides surface interaction.

In the present work, the platinum based alumina-supported catalysts modified or promoted by magnesia and bare magnesia were prepared by wet impregnation and used for the hydrogenation of N-(2`,3`-dimethoxy benzyl)-3,4-dioxy-methylene-phenylethylamine, This paper mainly to solve the instead of Raney nickel by support platinum catalysts, the effect of MgO on the structure properties, the reducibility, and the interaction of the Pt-Mg-Al oxides in the catalysts.

MATERIALS AND METHODS

Preparation of catalysts

The Pt/Al_2O_3 catalysts used in this study were prepared by the wet impregnation method, The commercial Al_2O_3 particles were calcinded at 500℃ for 3 h to increase pore volume and surface area, and then the Al_2O_3 particles were impregnated with an aqueous solution of $Mg(NO_3)_2 \cdot 6H_2O$ at room temperature for 10 h, rest 3 h, evaporated at 80℃, dried at 120℃ for 3 h, and then impregnated with aqueous solution of H_2PtCl_6, maintain magnetic stirring 10 h (500 RPM), ultrasonic oscillation 30 min, still 3 h, the platinum loading was 0.5wt% with H_2PtCl_6 as precursor. The samples were calcined after drying in the muffle furnace at 500℃ for 3 h, the precursors were then reduced in hydrogen (H_2/N_2) with a flow rate of 50 mLmin^{-1}, held at 400℃ for 6 h, and then cooled to the room temperature in argon atmosphere for experiments or further characterization. The different amount of MgO on the catalysts were loaded by changing the concentration of $Mg(NO_3)_2 \cdot 6H_2O$ of aqueous solution in the procedure of impregnation, the loading amount of Pt was 0.5 wt%, whereas the loading amount of MgO was varied (x=0, 2, 4, 6, 8 ,10 wt%), and Al_2O_3 maintained 10 g, respectively, the catalysts were denoted as 0.5 Pt/Al_2O_3-xMgO, the reagents used are all of analytical grade. The Pt/MgO catalysts were also prepared with the same sequential impregnation method by using aqueous solution of $Mg(NO_3)_2 \cdot 6H_2O$ and NaOH to get the precursor of MgO support, and then impregnated with aqueous solution of H_2PtCl_6, the platinum loading was 0.5 wt% with H_2PtCl_6 as precursor.

Characterization of the catalysts

BET

N_2 adsorption/desorption isotherms of the catalysts were obtained in a Builder SSA-4200 adsorption instrument using N_2 as the adsorbent. The amount of catalysts used was 150 mg, prior to the measurement, the samples were out-gassed at 150℃ under N_2 flow for 6 h, then, the specific surface area, pore volumes and pore sizes were analyzed by N2 physisorption at -200℃, the results were analyzed by the Brunnauer-Emmett-Teller (BET) method.

XRD

The surface phase composition was studied by X-ray diffraction (XRD, D8 advanced) using Cu Kα radiation, the tube voltage was 40 kV, and the current was 30 mA. The samples were scanned over 2θ=2-80° at a ramp rate of 0.06°/s.

CO₂-TPD

The basicity of the calcined samples was determined by carbon dioxide temperature programmed desorption (CO_2-TPD) in an AutoChem II 2920 Chemisorption analyzer, approximately 200 mg of each tested samples was placed in the reaction tube, after pretreatment at 450℃ for 1 h under a He flow of 30 mL/min., the sample was cooled to 100℃ and then reacted with flowing CO_2 under isothermal conditions and subsequently cooled to room temperature, the CO_2-TPD was then performed with a ramp of 8℃.min^{-1} from 100℃ to 800℃ under a He atmosphere.

TEM

The morphology of the catalysts after reduction was determined by transmission electron microscopy (TEM, JEM2010), the samples were mixed with alcohol and deposited on a Cu grid covered with a perforated carbon membrane.

H₂-TPR

The optimum reduction temperature of the catalysts was determined by temperature programmed reduction of hydrogen (H_2-TPR) in an AutoChem II 2920 Chemisorption analyzer, approximately 200 mg of each tested samples was placed in the reaction tube, the temperature was programmed to ramp at 8℃.min^{-1} to 400℃ and hold for 30 min

under a Helium atmosphere, then ,the samples was cooled to 100℃, subsequently, the gas line was switched to $H^2/$ Ar, after the baseline was stable, the programmed reduction of H_2 was run from 100℃ to 800℃ with a heating rate of 8℃.min^{-1}.

XPS

The elemental compositions of the catalyst surface were identified by X-ray Photoelectron Spectrometer (XPS, PHI 5000 Versaprobe) equipped with Mg-Ka radiation, the binding energies were referenced to the C1s band at 284.6 eV.

Catalytic test

The obtained catalysts with different MgO load were used for the hydrogenation of Shiff's base with H_2 to produce precursor of Berberine Hydrochloride using a high-pressure agitated autoclave with 500 mL capacity. The autoclave was filled with 0.6 g of catalysts and 180 mL of absolute methanol containing 125 mL of Shiff's base, and was flushed with hydrogen more than three times at room temperature. The reaction was carried out at 85℃-115℃ and 1-4 MPa hydrogen partial pressures for 2 h. the solution was cooled down to room temperature and centrifuged to remove the solid catalysts. The liquid product was collected and the crystal product obtained by crystallization.

RESULTS AND DISCUSSION

BET results

N_2 adsorption-desorption analysis of the catalysts were conducted using an automated gas sorption analyzer, the surface areas and pore volume were obtained by BET methods, respectively. **Table 1** shows that the BET surface area, pore volume, and average pore diameter of the catalysts. It can be seen in **Table 1**, the 0.5 Pt/Al_2O_3 samples exhibits the highest BET surface area of 93.196 m²/g among the catalysts with or no loading of MgO, but the Pt/MgO catalysts were 15.6 times of pore volume, 2.5 times of surface area (BJH), and 2.5 times of pore diameter as large as Pt/Al_2O_3, it was indicated that the mesoporosity of MgO was stronger than the bare Al_2O_3 support. The textural properties of $0.5Pt/Al_2O_3$-xMgO have no significant change with addition of MgO, especially in pore diameter.

Table 1: Textural properties of the catalysts.

Catalysts	Surface area (BET) (m²/g)	Pore volume (cm³/g)	Surface area (BJH) (cm³/g)	Pore diameter (nm)
$0.5Pt/Al_2O_3$	93.196	0.048	26.053	10.548
$0.5Pt/Al_2O_3$-	88.839	0.047	24.973	10.724
$0.5Pt/Al_2O_3$-4MgO	78.234	0.048	23.913	10.701
$0.5Pt/Al_2O_3$-6MgO	76.487	0.042	21.452	10.723
$0.5Pt/Al_2O_3$-8MgO	74.189	0.039	20.051	10.865
$0.5Pt/Al_2O_3$-10MgO	70.171	0.037	18.067	10.568
$0.5Pt/MgO$	57.417	0.751	65.458	26.201

XRD results

The XRD patterns of the catalysts with different MgO loading were shown in **Figure 1**.According to the literature, the diffraction peaks at 36.7º, 39.4º, 45.7º, and 66.4º represent Al_2O_3 crystal planes, 36.5º, 43.0º, 62.3º, 74.7º, and 78.6º represent MgO crystals plane, 39.8º, and 46.2º represent Pt metal atom crystal plane. It can be observed in the **Figure1(1)** that the diffraction peaks at 18.9º, 37.78°, 51.8°, 57.50°and 62.3º represent the combination phases of α- Al_2O_3 and γ- Al_2O_3 as a results of the calcination temperature at 500℃, and the shift of the diffraction peaks implied that the strong interaction exhibited in Pt species with the Al_2O_3 support. With addition of MgO from **Figure 1(2)** to **Figure 1(6),** the typical diffraction peaks of MgO crystal plane clearly exhibited, and the weak diffraction peaks at 37.0º, 38.4º, and 57.50º attributed to the weak interaction of MgO with Al_2O_3, it was indicated that the MgO was uniformly dispersed on the strong Al2O3 support attributed to the strong interaction of the chloroplatinic acid (H2PtCl6) with the MgO. The **Figure 1(7)** showed that intensity of the diffraction peaks at 43.0º, 62.3º,

74.7º and 78.6º were stronger more than that from **Figure 1(2)** to **Figure 1(6)**, and the weak diffraction peaks at 39.8º, and 46.2 º represent Pt metal atom, it was indicated that the Pt particles were better dispersed on the bare MgO support.
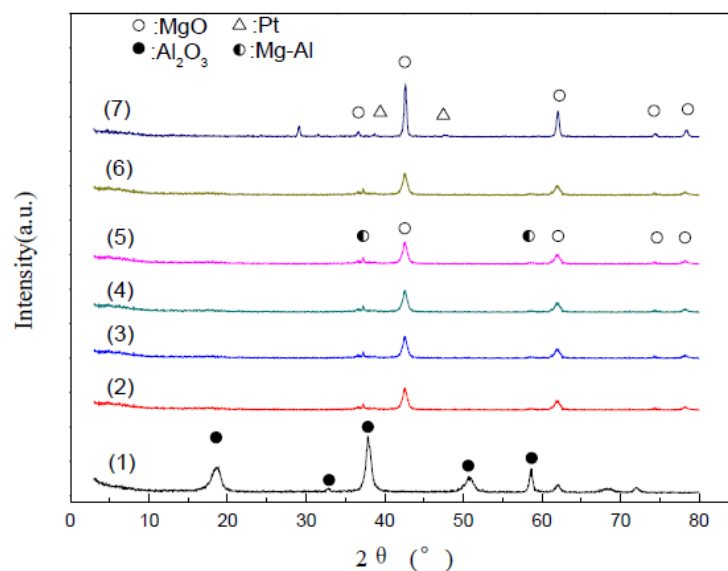
Figure 1: ^{1}H NMR spectrum of the title compound in DMSO-d$_6$.

TEM results

The TEM image of the catalysts with different MgO loading amount were shown in **Figure 2**. It can be seen clearly in **Figure 2 (1)** that only the surface reduction of platinum taken place on the aggregation of species due to the strong interaction of chloroplatinic acid and the Al$_2$O$_3$ support. In **Figures 2 (2)** and **2 (3)**, some ruled and about 50 nm crystal existed with the addition of MgO, and much and more with MgO load, this is attributed to the neutralization of the basic MgO, and the dispersion of Pt cluster increased as the spinel structure of PtO- Al$_2$O$_3$ species produced. In **Figures 2 (4)-2 (6),** the interaction mainly taken placed between the MgO and chloroplatinic acid, and the dispersion of Pt was more increased. In **Figure 2 (7),** the bare MgO support exhibited sheet structure as the precursor of Mg(OH)$_2$ species, the average diameter of MgO supports were about 20-30 nm,the Pt cluster dispersed uniformly.
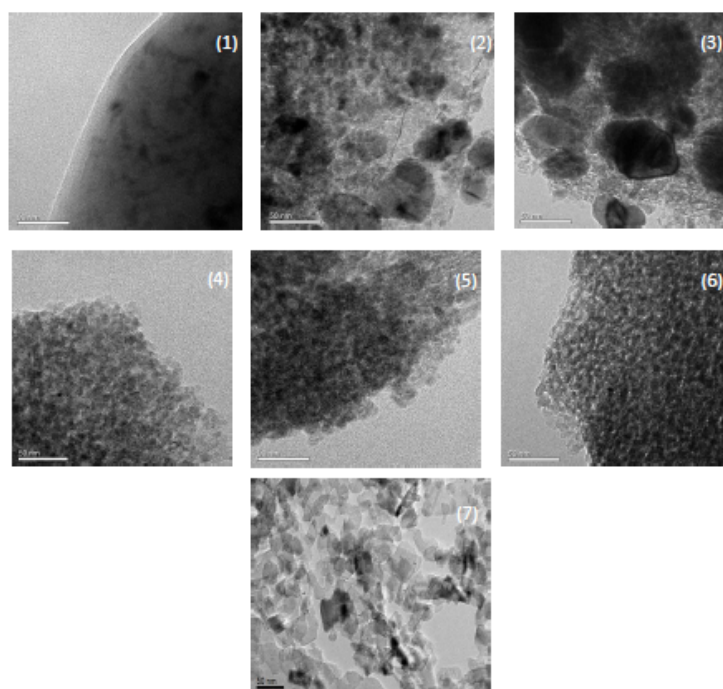

Figure 2: ^{13}C NMR spectrum of the title compound in DMSO-d$_6$.

H$_2$-TPR

The **Figure 3** presents the H2-TPR profiles of the catalysts with different MgO loading amount. There were two reduction peaks obtained in the bare Pt/Al$_2$O$_3$ catalysts in **Figure 3 (1),** the reduction temperature of Pt/Al$_2$O$_3$ catalyst at 160 °C was assigned to the reduction of Pt^{4+} in the usually classified PtO$_2$ species as the precursors were calcined at 500°C, and over 600°C was attributed to the deposited in the support or the reduction of the hydroxyl in Al$_2$O$_3$ support, it indicated that the strong interaction exhibited between the precursor of (PtOCl) species and Al$_2$O$_3$ support [29], the weak and negative intensity of Pt/Al$_2$O$_3$ catalyst implied that only surface Pt particles reduction existed as a result of the strong interaction or the PtO$_2$ species deposited in the support. In **Figures 3(2)-3(4)** with 2-6 wt% MgO load, it can be seen that the reduction temperature at low temperature reduction zone increased and decreased at high temperature reduction zone, and the intensity of Pt/Al$_2$O$_3$ catalyst increased simultaneously and reached the highest value as 6 wt% MgO load, this was attributed to the strong interaction between the MgO and (PtOxCly) species and the weak interaction between MgO and Al$_2$O$_3$ support. In **Figure 3 (5)** with 8 wt% MgO load, there were fourth reduction peaks existed and the intensity of high reduction temperature zone increased, and the reducible Pt clusters increased, this was attributed to the neutralization of MgO and (PtOxCly) species. In **Figure 3 (6)** with 10 wt% MgO load, the intensity of low reduction temperature zone increased than 8 wt% MgO load relatively, it was indicated that more MgO load can decrease the strong acid effect on the Al2O3 support, and the dispersion of the Pt species increased as more MgO loading amount. In **Figure 3 (7)** with bare MgO support, the reduction peaks at high reduction temperature zone decreased and the intensity of Pt/MgO catalysts was ten times about Pt/Al$_2$O$_3$ catalysts, but the reduction temperature at low reduction temperature zone increased slightly, this was attributed to the Pt clusters enlarged as a result of flake H)$_2$ precursor.

CO$_2$-TPD

The obtained CO$_2$-TPD profiles of the catalysts with different MgO loading amount were shown in **Figure 4**. It can be seen that CO$_2$ desorbing in the different temperature ranges from 120°C to 250°C, 250°C to 350°C, even more than 350°C in **Figure 4**, this was attributed to the desorption peaks on the weak acid site, medium strong acid site and strong acid site, respectively. The desorption peaks at 160°C, 250°C, and 520°C were obtained in **Figures 4 (2)-4 (6)** with addition of MgO, and the temperature of

desorption peaks shifted left with the increased MgO load, with increase addition to 10 wt% MgO, the content in the catalysts results in a shift of the CO$_2$ desorption peak to lower temperature, which is indicative of a shift in surface basicity of the catalysts. This suggests that Mg^{2+} in the catalysts contribute to strong basic sites, and the difference of surface basicity can be attributing to the changes of Mg/Al ratio. The total quantity of basic reached maximum as the bare MgO support and the desorption temperature reached the lowest relatively in **Figure 4 (7).**

XPS

XPS was used to determine the surface platinium and ion species in the synthesized catalysts samples, the Pt 4f$_{7/2}$ XPS spectra of the catalysts supported on MgO was shown in **Figure 5**, in the Pt 4f$_{7/2}$ spectra, the peaks at around 529.57, 530.42 and 531.17 eV were attribute to the Pt particles and PtO$_2$ species, the binding energy of the Pt particles and PtO$_2$ species implied that the weak interaction existed between Pt particles and MgO support, on the other hand, the closed to binding energy indicated that the

some electron drawing group existed nearby Pt particles on the surface of the Pt/MgO catalysts The effects of obtained catalysts with different MgO load were tested, the conversion and the selectivity for the catalytic hydrogenation of N-(2`,3`-dimethoxy benzyl) -3,4-dioxy-methylene –phenylethylamine (Shiff's base) were summarized in **Table 2**. It can be seen that the Pt/MgO catalyst gave the highest selectivity and yield, this might attributed to the electron-deficient Pt surface favoring the adsorption of aromatic ring of Shiff's base as a result of the lateral repulsion of large molecules among adsorption [6], appropriate mesoporosity for large molecules, appropriate surface acidity and basicity of support for Shiff's base and H$_2$ are also to the benefit of catalytic reaction.
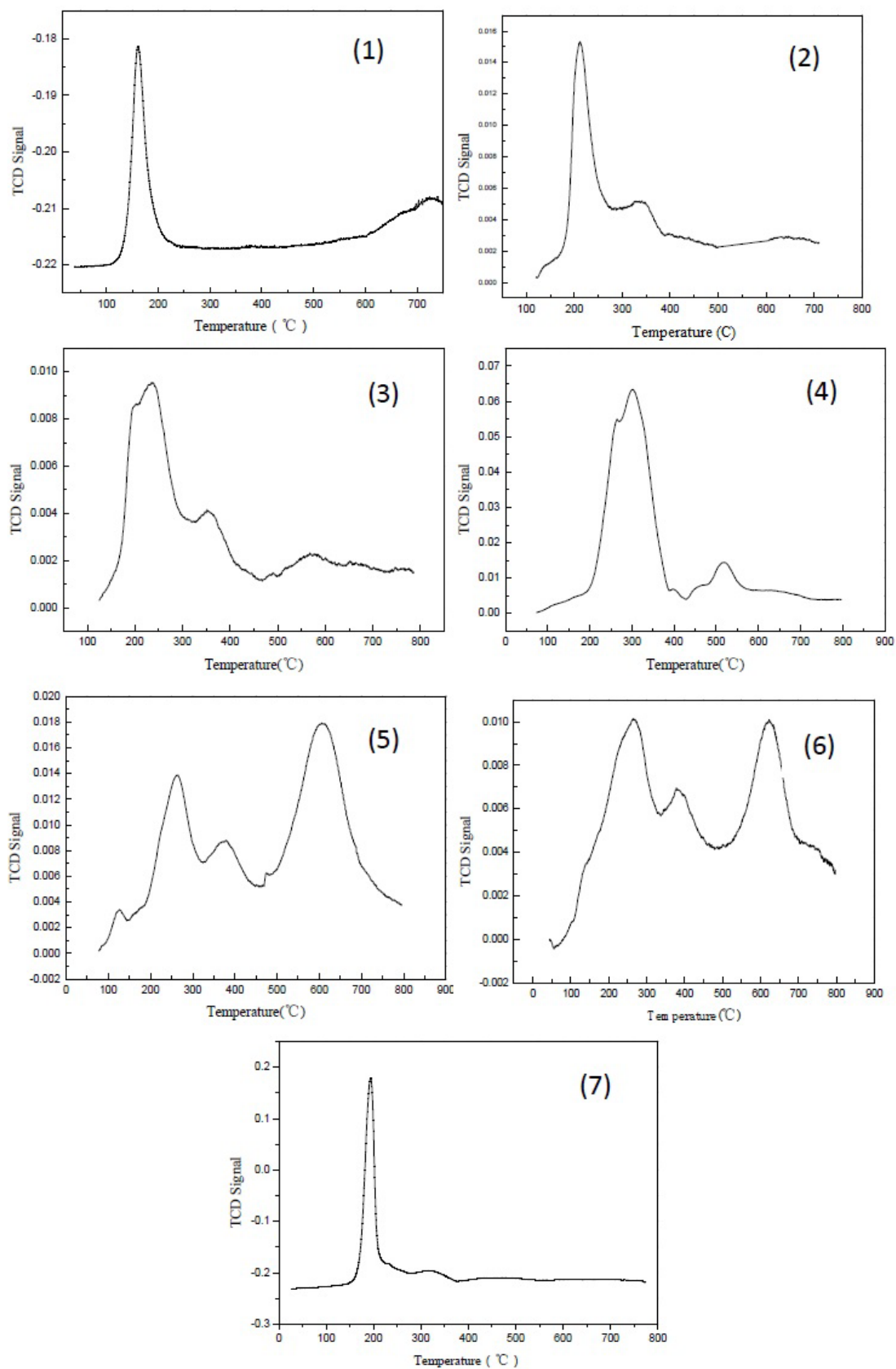
Figure 3: The H$_2$-TPR profiles of the catalysts with different MgO loading amount (0.5Pt/Al$_2$O$_3$-xMgO: x, wt%: 0, 2, 4, 6, 8, 10, 100).
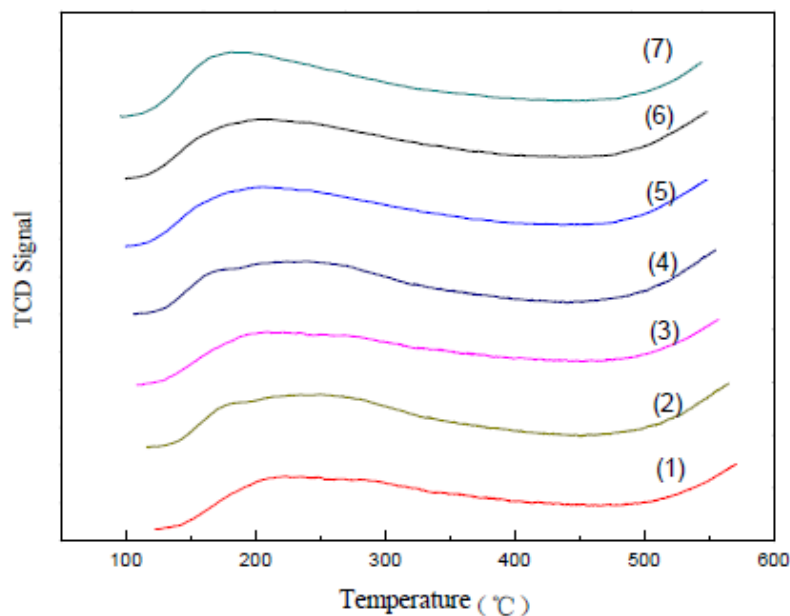
Figure 4: CO$_2$-TPD profiles of the catalysts with different MgO load (0.5Pt/Al$_2$O$_3$-xMgO: x, wt%: 0, 2, 4, 6, 8, 10, 100).
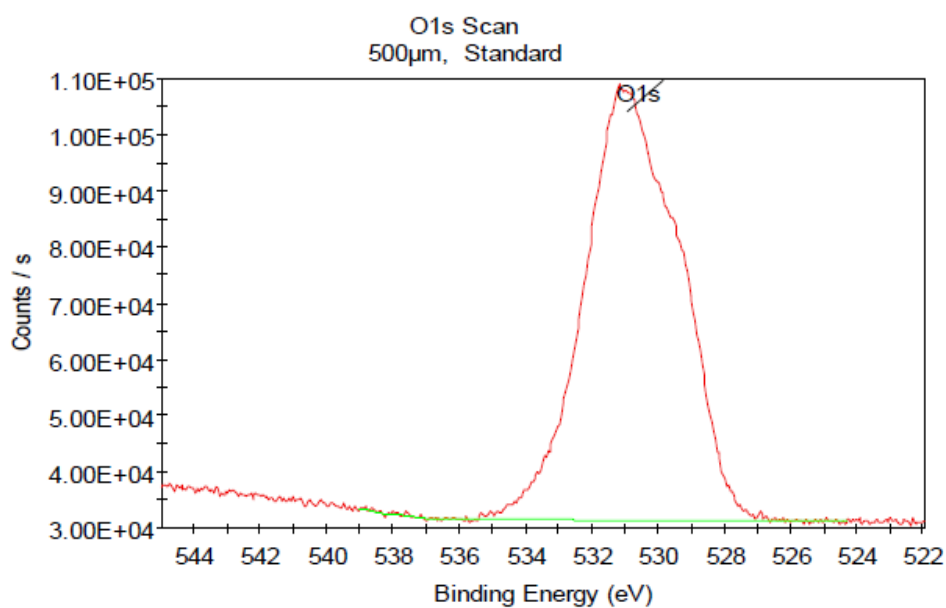

Figure 5: XPS spectra of the catalysts as bare MgO support

Table 2: The conversion and selectivity of the reaction with different MgO load.

Catalysts 0.5Pt/Al$_2$O$_3$-xMgO(x, wt %)	Conversion %	Selectivity %	Yields %
0.5Pt/Al$_2$O$_3$	72.84	80.81	58.86
0.5Pt-2MgO/Al$_2$O$_3$	75.43	83.85	63.24
0.5Pt-4MgO/Al$_2$O$_3$	75.98	84.89	64.50
0.5Pt-6MgO/Al$_2$O$_3$	78.43	86.87	68.13
0.5Pt-8MgO/Al$_2$O$_3$	83.94	89.81	75.38
0.5P-10MgO/Al$_2$O$_3$	88.02	91.76	80.76
0.5Pt/MgO	96.74	95.25	92.14

CONCLUSION

Pt/Al$_2$O$_3$, Pt/Al$_2$O$_3$-xMgO and Pt/MgO catalysts were studied for hydrogenation of N-(2`,3`-dimethoxy benzyl)-3,4-dioxy-methylene-phenylethylamine, the physical properties of the catalysts, the surface acidity or basicity of the support, the interaction of active particles with support, the reducibility, dispersion, and active surface area of Pt for the prepared catalysts were studied by the N$_2$ physi-sorption, X-ray Diffraction (XRD), Carbon Dioxide Temperature Programmed Desorption (CO$_2$-TPD), Transmission Electron Microscopy (TEM), Temperature Programmed Reduction of Hydrogen (H$_2$-TPR), and X-ray Photoelectron Spectrometer (XPS). The results indicated that the basic support (MgO) caused the electron deficient surface metallic Pt that favored the hydrogenation of N-(2`,3`-dimethoxy benzyl)-3,4-dioxy -methylene-phenylethylamine, and the mesoporosity of MgO support was benefit for the transport of large molecules reactants and products. The utilization of meso-porous Pt/MgO for catalytic hydrogenation of N-(2`,3`-dimethoxy benzyl)-3,4-dioxy-methylene-phenylethylamine (Shiff's base) with the highest conversion of 96.74%, the highest selectivity of 95.25% and yields of 92.14%, it confirmed that the instead of Raney Ni was feasible.

REFERENCES

[1] Kirgilin A, Wärnå J, Tokarev A, Dmitry Yu, Murzin (**2014**) Kinetic modeling of sorbitol aqueous-phase reformin over Pt/Al$_2$O$_3$. *Ind Eng Chem Res* 53: 4580-4588.

[2] Shabaker JW, Dumesic JA (**2004**) Kinetics of aqueous-phase reforming of oxygenated hydrocarbons: Pt/Al$_2$O$_3$ and Sn-Modified Ni Catalysts. *Ind Eng Chem Res* 43: 3105-3112.

[3] Wasylenko W, Frei H (**2005**) Direct observation of surface ethyl to ethane interconversion upon C$_2$H$_4$ Hydrogenation over Pt/Al$_2$O$_3$ catalyst by time-resolved FT-IR Spectroscopy. *J Phys Chem* 109: 16873-16878.

[4] Lira E, Merte LR, Behafarid FLK, Ono LZ, Cuenya BR (**2014**) Role and evolution of nanoparticle structure and chemical state during the oxidation of no oversize- and shape-controlled Pt/γ- Al$_2$O$_3$ Catalysts under Operando Conditions. *ACS Catal* 4: 1875-1884.

[5] Stakheev AY, Zhang Y, Ivanov AV, Baeva GN, Ramaker DE, et al. (**2007**) Separation of geometric and electronic effects of the support on the co and h2 chemisorption properties of supported pt particles: the effect of ionicity in modified alumina supports. *J Phys Chem* 111: 3938-3948.

[6] Moses-debusk M, Yoon M, Allard LF, David R, Mullins, et al. (**2013**) CO oxidation on supported single Pt atoms: experimental and ab initio density functional studies of CO interaction with Pt atom on θ-Al2O3(010) surface. *J Am Chem Soc* 135: 12634-12645.

[7] Climent MJ, Corma A, Iborra S, Marti L (**2015**) Process intensification with bifunctional heterogeneous catalysts: Selective One-Pot Synthesis of 2′-Aminochalcones. *ACS Catal* 5: 157-166.

[8] Wolf D, Markus H, Baerns M (**1997**) External mass and heat transfer limitations of the partial oxidation of methane over a Pt/MgO Catalyst consequences for adiabatic reactor operation. *Ind Eng Chem Res* 36: 3345-3353.

[9] Nimmanwudipong T, Runnebaum RC, Brodwater K, Jennifer H, Block DE, et al. (**2014**) Design of a High-Pressure Flow-Reactor System for Catalytic Hydrodeoxygenation: Guaiacol Conversion Catalyzed by Platinum Supported on MgO. *Energy Fuels* 28: 1090-1096.

[10] Lee SW, Ihm SK (**2013**) Characteristics of Magnesium-Promoted Pt/ZSM-23 Catalyst for the Hydroisomerization of n-Hexadecane. *Ind Eng Chem Res* 52: 15359-15365.

[11] Redekop EA, Galvita VV, Poelman H, Bliznuk V (**2014**) Delivering a Modifying Element to Metal Nanoparticles via Support: Pt–Ga Alloying during the Reduction of Pt/Mg(Al,Ga)Ox Catalysts and Its Effects on Propane Dehydrogenation. *ACS Catal* 4: 1812-1824.

[12] Shuang L, Xiaodong W, Duan W, Rui R (**2012**) NOx-Assisted Soot Oxidation on Pt–Mg/Al2O3 Catalysts: Magnesium Precursor, Pt Particle Size, and Pt–Mg Interaction. *Ind Eng Chem Res* 51: 2271-2279.

[13] Aramendía MA, Benítez JA, Borau V, Jimenze C, Marinas JM (**1999**) Study of MgO and Pt/MgO Systems by XRD, TPR, and 1H MAS NMR. *Langmuir* 15: 1192-1197.

[14] Alexeev O, Kawi S, Shelef M, Gates BC (**1996**) Synthesis and Characterization of Model MgO-Supported Catalysts with Pt−Mo Interactions. *J Phys Chem* 100: 2066-2068.

[15] Bokhimi, Aceves A, Novaro O, Lopez T (**1995**) Pt Effect on the Particle Morphology and Crystalline Structure of Pt/MgO Catalysts *J Phys Chem* 99: 14403-14406.

[16] Lopez N, Francesc I (**1998**) Ab Initio Modeling of the Metal-Support Interface: The Interaction of Ni, Pd, and Pt on MgO(100). J Phys Chem B 102: 1430-1436

[17] Grunbeck H, Broqvist P (**2003**) CO-Induced Modification of the Metal/MgO(100) Interaction. *J Phys Chem B* 107: 12239-12243.

[18] Hejral U, Vlad A, Nolte P (**2013**) Stierle A.In Situ Oxidation Study of Pt Nanoparticles on MgO(001). *J Phys Chem C* 117: 84-88.

[19] Kozlov SM, Aleksandrov HA, Neyman KM (**2015**) Energetic Stability of Absorbed H in Pd and Pt Nanoparticles in a More Realistic Environment. *J Phys Chem C* 119: 5180-5186.

[20] Kozlov SM, Aleksandrov HA, Neyman KM (**2014**) Adsorbed and Subsurface Absorbed Hydrogen Atoms on Bare and MgO(100)-Supported Pd and Pt Nanoparticles. *J Phys Chem C* 118: 15242-15250.

[21] Ahmad R, Singh AK (**2015**) Pt-Poisoning-Free Efficient CO Oxidation on Pt3Co Supported on MgO(100): An Ab Initio Study. *ACS Catal* 5: 1825-1832.

[22] Noda S, Masateru N, Azuchi H, Masayoshi S (**1998**) Gas-Phase Hydroxyl Radical Generation by the Surface Reactions over Basic Metal Oxides. *J Phys Chem B* 102: 3185-3191.

[23] Copeland JR, Santillan IA, Schimming MN, Ewbank JL, Sievers C (**2013**) Surface Interactions of Glycerol with Acidic and Basic Metal Oxides. *J Phys Chem C* 117: 21413-21425.

[24] Costas NC, Efstathiou AM (**2007**) Mechanistic Aspects of the H2-SCR of NO on a Novel Pt/MgO−CeO2 Catalyst. *J Phys Chem C* 111: 3010-3020.

[25] Chi Y, Steven SC (**2000**) Infrared and TPD studies of nitrates adsorbed on Tb4O7, La2O3, BaO, and MgO/γ-Al2O3. *J Phys Chem B* 104: 4673-4683.

[26] Prinetto F, Ghiotti G, Nova I, Lietti L, Tronconi E (**2001**) FT-IR and TPD Investigation of the NOx Storage Properties of BaO/Al2O3 and Pt−BaO/Al2O3 Catalysts. *J Phys Chem B* 105: 12732-12745.

[27] Frola F, Manzoli M, Prinetto F, Ghiotti G (**2008**) Pt-Ba/Al2O3 NSR Catalysts at Different Ba Loading: Characterization of Morphological, Structural, and Surface Properties. *J Phys Chem C* 112: 12869-12878.

[28] Virnovskaia A, Morandi S, Erling R, Giovanna G, Olsbye U (**2007**) Characterization of Pt,Sn/Mg(Al)O Catalysts for Light Alkane Dehydrogenation by FT-IR Spectroscopy and Catalytic Measurements. *J Phys Chem C* 111: 14732-14742.

[29] Zhimin L, Xiaohong L, Zhijian C, Pinliang Y, Li Chan, et al. (**2009**) Effect of reduction method on the surface states of Pt/Al2O3. *Energy Fuels* 37: 205-207.